

# Simultaneous Magneto-Optical Trapping of Bosonic and Fermionic Chromium Atoms

R. Chicireanu, A. Poudereux, R. Barbé, B. Laburthe-Tolra, E. Maréchal, L. Vernac, J.-C. Keller, and O. Gorceix

*Laboratoire de Physique des Lasers, UMR 7538 CNRS,  
Université de Paris Nord, 99 Avenue J.-B. Clément, 93430 Villetaneuse, France*

(Dated: April 18, 2018)

We report on magneto-optical trapping of fermionic  $^{53}\text{Cr}$  atoms. A Zeeman-slowed atomic beam provides loading rates up to  $3 \times 10^6 \text{ s}^{-1}$ . We present systematic characterization of the magneto-optical trap (MOT). We obtain up to  $5 \times 10^5$  atoms in the steady state MOT. The atoms radiatively decay from the excited P state into metastable D states, and, due to the large dipolar magnetic moment of chromium atoms in these states, they can remain magnetically trapped in the quadrupole field gradient of the MOT. We study the accumulation of metastable  $^{53}\text{Cr}$  atoms into this magnetic trap. We also report on the first simultaneous magneto-optical trapping of bosonic  $^{52}\text{Cr}$  and fermionic  $^{53}\text{Cr}$  atoms. Finally, we characterize the light assisted collision losses in this Bose-Fermi cold mixture.

PACS numbers: 32.80.Pj, 39.25.+k, 42.50.Vk

## INTRODUCTION

Although laser cooling generally assumes the presence of an almost closed transition [1], it is now possible to laser cool in a magneto-optical trap (MOT) atomic species whose internal level structure is more complex than that of alkali atoms. A more complex electronic structure may lead to qualitatively new physics. In the case of  $^{52}\text{Cr}$ , for example, for which Bose-Einstein condensation was reached recently in the group of T. Pfau in Stuttgart, Germany [2], anisotropic, long-range dipole-dipole interactions play a visible role in the expansion of the BEC after it is released from its trap [3] - contrary to all previous experimental data on BECs, for which all interaction effects could be modeled by short-range isotropic interactions. In addition, the optical manipulation of new atoms may find technical applications, which is the case for chromium (Cr) [4], but also for example, for group III atoms (such as Al, Ga, In) and for Fe [5].

The optical manipulation of species with complex electronic structure can nevertheless be a technical challenge when the cooling transition is not closed, since more and more repumping lasers are then needed. For example, laser cooling of molecules has never been investigated because of the many vibrational levels associated with a given electronic transition. Here, we report on the magneto-optical trapping of fermionic  $^{53}\text{Cr}$  atoms. As with bosonic  $^{52}\text{Cr}$  atoms, the cooling transition is not perfectly closed and atoms are depumped towards metastable dark states, so that two repumpers are required to effectively close this transition. In addition, and in contrast to  $^{52}\text{Cr}$  which has no hyperfine structure,  $^{53}\text{Cr}$  nuclear magnetic moment is  $I = 3/2$ , and its electronic ground state has four hyperfine components. Further repumpers are therefore needed, to prevent optical pumping towards dark hyperfine states.

Obtaining a MOT for  $^{53}\text{Cr}$  atoms is appealing for several reasons. Starting from a laser-cooled atomic vapor,

it has been possible to reach quantum degeneracy for nine bosonic atomic species, which is one of the major achievements of atomic physics in the last ten years. However, up to now only two fermionic species,  $^{40}\text{K}$  and  $^6\text{Li}$ , were cooled down to quantum degeneracy [6]. For both species, it was possible to reach the strongly interacting regime by use of Feshbach resonances, and to study the cross-over between the BCS and the BEC regimes. It is therefore interesting to add a new species in the ultra-cold fermionic playground. The main specificity of chromium is its large magnetic moment of  $6 \mu_B$ : in polarized degenerate Fermi seas, dipole-dipole interactions will be the leading interaction term, which is expected to produce new quantum phases [7]. In addition, the atomic ground state hyperfine structure together with its strong magnetic dipole moment should lead to a rich Feshbach resonances spectrum. Finally we report in this paper that it is possible to simultaneously trap  $^{53}\text{Cr}$  and  $^{52}\text{Cr}$  atoms, and discuss the perspectives to produce chromium Bose-Fermi mixtures in the quantum regime.

## EXPERIMENTAL SETUP

### Laser system

Figure 1 shows a simplified energy-level diagram for  $^{52}\text{Cr}$  and  $^{53}\text{Cr}$  atoms. The  $^7\text{S}_3 \rightarrow ^7\text{P}_4$  transition ( $\lambda = 425.51 \text{ nm}$ , natural linewidth  $\gamma/2\pi = 5.02 \text{ MHz}$ , saturation intensity  $I_s = 8.52 \text{ mW.cm}^{-2}$ ) is used both to decelerate the two isotopes in a Zeeman slower, and to cool and trap them in a MOT. Since no suitable diode laser source is yet available at 425 nm, we generate 350 mW of blue laser light by frequency doubling high-power light at 851 nm using a non-linear 8 mm long LBO crystal in a resonant optical cavity. The light at 851 nm is produced with an argon-ion laser (10.5 W) pumping a commercial Ti:Sapphire laser from Tekhnoscan. The infrared power output is typically 1.3 W. The frequency

of the Ti:Sa laser is stabilized by locking it to a Fabry-Perot (FP) reference cavity (whose finesse is 100). The FP spacer is made of Invar steel. The cavity is housed in an evacuated chamber, which is isolated acoustically and thermally. The length of the Fabry Perot cavity is locked to the  ${}^7S_3 \rightarrow {}^7P_4$  transition of  ${}^{52}\text{Cr}$  by use of a standard saturation spectroscopy setup on an hollow cathode lamp. The doubling cavity is kept in resonance with the infra-red light using a Hänsch-Couillaud locking technique [8]. We estimate the blue laser jitter to be around one MHz. Several Acousto-Optic Modulators (AOMs) are necessary to generate the laser frequencies needed for slowing and trapping both chromium isotopes (see Fig 1).

The  ${}^7S_3 \rightarrow {}^7P_4$  transition is slightly leaky since excited atoms can decay from  ${}^7P_4$  to dark  ${}^5D$  states (see Fig 1 and [11]). To compensate for that effect, repumping lasers can be used to pump atoms from the metastable D states back to the ground  ${}^7S_3$  state via the  ${}^7P_3$  state. Their wavelength are in the range of 660 nm and are thus referred as the 'red' repumpers in the following. In our setup they are produced by external cavity laser diodes, each locked to the Fabry-Perot reference cavity using a Pound-Drever-Hall scheme [12].

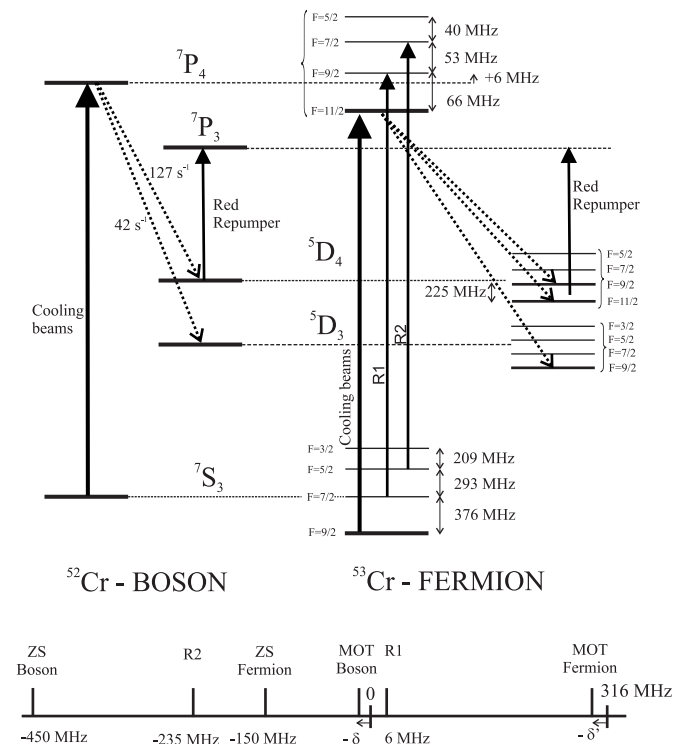


FIG. 1: Relevant energy levels for cooling and trapping  ${}^{52}\text{Cr}$  and  ${}^{53}\text{Cr}$  including the leaks to metastable states and (bottom) sketch of the laser frequencies used in our experiment ( $\delta$  and  $\delta'$  stand for the MOT detunings). Transition probabilities to the bosonic metastable states are from [9], hyperfine structure splitting of the fermionic isotope are from [10]. We deduced from our experiment the isotopic shift between the  ${}^{52}\text{Cr}$   ${}^7S_3 \rightarrow {}^7P_4$  transition and the  ${}^{53}\text{Cr}$   $F = 7/2 \rightarrow F' = 9/2$  transition to be  $6 \pm 1$  MHz.

## The Chromium Source

Our chromium oven is a commercial Addon high temperature effusion cell. The realization of a robust chromium source is a technical challenge. Indeed, chromium is a very refractory metal, with a melting point of 1857 Celsius. Furthermore, Cr tends to react with most of the materials used to construct high temperature ovens. For example, direct contact with Tantalum (Ta) or Tungsten (W) must be avoided because Cr forms alloys with low temperature melting with them.

In our setup, the cell is resistively heated with two self supporting W filaments. The main crucible is in Ta. A chromium bar of 20 g (99.7 percent pure) is enclosed in a second crucible made of ultra pure alumina, which is inserted inside the Ta crucible. The temperature is measured with a W/Re thermocouple. A water cooled thermal shield maintains the vacuum chamber at a moderate temperature of 40 Celsius. The effusive source is terminated by a 2 mm diameter aperture. A 4 mm diameter aperture, set at a distance of 5 cm from the emission point, defines the direction of the atomic beam. The cell works in the horizontal plane and is connected to the chamber through a CF40 orientable flange. This provides the necessary fine tuning for the orientation of the atomic beam in order to align the thermal beam along the axis of the one meter long Zeeman slower tube. The atomic beam can be switched off and on within 200 ms with a mechanical shutter. The oven chamber is pumped with a  $250 \text{ L.s}^{-1}$  turbo-pump. We usually work with an oven at a temperature of 1500 Celsius, and the pressure in the oven chamber is then equal to  $3 \times 10^{-10}$  mbar.

## The Zeeman Slower

A Zeeman slower (ZS) connects the oven chamber to the MOT chamber. It is made of three sets of copper coils wrapped around a one-meter-long steel tube, which has an internal diameter of 1.4 cm, and is connected to the oven chamber through a 10 cm-long flexible hose. At the entrance of the ZS tube, a 25 cm-long differential pumping tube having a 0.9 cm internal diameter allows limiting pressures in the experimental chamber below  $5 \times 10^{-11}$  mbar when the oven is on.

The experimental magnetic field profile achieved is a usual positive- to- negative square root profile, allowing one to get a well-defined final velocity (see [13] for a discussion on the extraction at the end of a ZS, and [14] for a recent and detailed paper on a ZS). It consists in three parts: the "branching zone" at the beginning of the tube where the magnetic field rises and quickly reaches its maximum intensity  $B_{max} > 0$ ; the "slowing zone" with a smooth decrease towards  $B_{min} < 0$ ; and a "final decrease zone" from  $B_{min}$  to zero (these three zones are shown in the insert of Fig 2). The small diameter of the

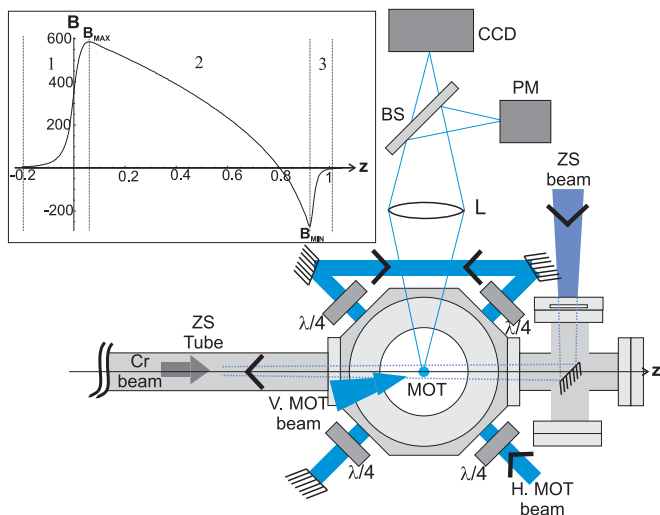


FIG. 2: Schematic of the experimental chamber showing the MOT beams, the coupling of the ZS beam, and the MOT fluorescence detection.  $L$ , lens;  $\lambda/4$ , quarter waveplate; BS, beam splitter; V., vertical; H., horizontal. The insert shows a plot of the experimental ZS magnetic field in G as a function of the  $z$  position along its axis in m. See text for a discussion of the three zones.

final coil makes it possible to obtain a short "final decrease zone". This allows us to produce the MOTs close to the exit of the tube (10 cm), which reduces losses due to transverse expansion at the end of the slower. The experimental magnetic B field values are  $B_{max} = 460$  G and  $B_{min} = -260$  G, which, together with the detuning of the ZS laser beam ( $-450$  MHz), define a capture velocity  $V_c$  of  $460 \text{ m.s}^{-1}$ , and a final velocity of  $40 \text{ m.s}^{-1}$ .

At the exit of the oven, the populations of the fermionic isotope (respectively bosonic) are equally distributed into the 28 (7) Zeeman sublevels of the four (one) hyperfine ground states (ground state). Only the atoms reaching the "slowing zone" in the  $|F = 9/2, m_F = 9/2\rangle$  ( $m_J = 3$ ) Zeeman sublevel can be slowed down in the ZS. In order to get a theoretical estimate of the fluxes of atoms slowed in the ZS, we carried out optical pumping calculations for both the bosonic and fermionic isotopes. While the bosonic case is easy to deal with, the fermionic one is much more complicated. First the number of levels (28 in the  ${}^7S_3$  and 36 in the  ${}^7P_4$ ) is large. In addition, the Zeeman energy shifts become comparable with the hyperfine structure for low values of the B field (a few Gauss for the excited  ${}^7P_4$  state), so that the calculations must involve the true eigenstates, which are neither the hyperfine ( $F, m_F$ ) states nor the Zeeman ( $m_J, m_I$ ) states.

We found that most of the  ${}^{52}\text{Cr}$  atoms whose velocity is smaller than or equal to  $V_c$  are optically pumped into the  $m_J = +3$  state by the ZS slowing beam inside the "branching zone". On the contrary, no substantial accumulation in the  $|F = 9/2, m_F = 9/2\rangle$  state is expected for the  ${}^{53}\text{Cr}$  atoms as they travel through the "branching zone" (6% instead of  $3.5\% = 1/28$ ). Taking into account both this different behavior with respect

to optical pumping and the isotopic proportion in natural chromium, we expect the ratio of the flux of slowed  ${}^{53}\text{Cr}$  atoms to the flux of slowed  ${}^{52}\text{Cr}$  atoms to be equal to  $0.06 \times 9.5/84 = 0.7\%$ . The experimental ratio, deduced from the analysis of MOT loading sequences, is larger, almost equal to 2% at 1500 Celsius. It should be noted though that less laser power is available for the Boson manipulation than for the Fermion in our experiment.

In the ZS, the  ${}^{53}\text{Cr}$  atoms experience a bad crossing pattern: for  $B = 25$  G, the two excited eigenstates adiabatically connected respectively to  $|F' = 11/2, m_{F'} = 11/2\rangle$  and to  $|F' = 9/2, m_{F'} = 7/2\rangle$  at  $B = 0$  G are degenerate, so that any  $\sigma^-$  polarized ZS laser depumps the atoms towards the  $F = 7/2$  ground state. In our experiment we clearly do not expect the ZS laser beam to be perfectly  $\sigma^+$  polarized: we use an ultrahigh vacuum metallic Al mirror to reflect the ZS beam and align it along the chromium beam (see Fig 2); this mirror is coated by chromium as time goes on, and its reflectivity properties slowly change in time [15]. Optical pumping calculations show that about 20% of the atoms can be lost if 10% of the ZS power is  $\sigma^-$  polarized. To repump  ${}^{53}\text{Cr}$  atoms in the ZS, we use the  ${}^{52}\text{Cr}$  ZS beam, which is (at 25 G) resonant with the transition between the states adiabatically connected to  $|F = 7/2, m_F = 7/2\rangle$  and  $|F' = 9/2, m_{F'} = 9/2\rangle$  (at  $B = 0$  G). Experimentally we got the optimal  ${}^{53}\text{Cr}$  MOT loading rates with a power of 3 mW in the  ${}^{52}\text{Cr}$  ZS beam, and 30 mW in the  ${}^{53}\text{Cr}$  ZS beam. The  $1/e^2$  radius of the  ${}^{52}\text{Cr}$  ZS beam and of the  ${}^{53}\text{Cr}$  ZS beam is respectively 3 mm and 3.6 mm at the MOT position, and both beams are approximately focused at the oven position. The presence of the  ${}^{52}\text{Cr}$  ZS beam as a repumper in the fermionic Zeeman slower results in an increase of about 40% in the final number of atoms in the  ${}^{53}\text{Cr}$  MOT.

We also performed a standard 1D transverse cooling in the oven chamber along the horizontal direction, using a laser having the same frequency as the MOTs lasers. In order to compensate for the red detuning of these lasers we applied a B field of a few Gauss along the transverse cooling beam direction. In the optimal experimental configuration, the transverse cooling laser has a power of 10 mW, and induces a gain of 2 to 2.5 in the steady state MOT populations. Finally we obtained MOT loading rates of the order of  $1.6 \times 10^8$  ( $3 \times 10^6$ )  $\text{atoms.s}^{-1}$  for  ${}^{52}\text{Cr}$  ( ${}^{53}\text{Cr}$ ) at  $T = 1500 \text{ C}$ .

### The Experimental Chamber

Our experimental chamber is a compact octagonal chamber with eight CF40 viewports in the horizontal plane, and two CF100 viewports for the coupling of vertical laser beams (see Fig 2). A  $150 \text{ L.s}^{-1}$  ion pump and a Ti-sublimation pump maintain the pressure at about  $5 \times 10^{-11}$  mbar. Two horizontal external coils in anti-

Helmholtz configuration create a quadrupole field at the MOT position. The MOT laser beam setup uses two independent arms: a vertical beam is retroreflected, and a single horizontal retroreflected beam provides all four horizontal cooling beams (as shown in Fig 2). The atomic clouds are imaged both on a PhotoMultiplier (PM), and a CCD Camera with a 12.5 cm focal length lens.

## EXPERIMENTAL RESULTS

### Magneto-optical trapping of $^{52}\text{Cr}$ atoms

As a first step, we report the achievement of a magneto-optical trap with bosonic  $^{52}\text{Cr}$  atoms. After transverse optical cooling, the atoms are slowed in the ZS, and trapped in the MOT. Because  $^{52}\text{Cr}$  has no hyperfine structure, a single frequency is sufficient to slow the atoms in the ZS, and another to cool and trap atoms in a MOT. The vertical magnetic field gradient is 18  $\text{G}\cdot\text{cm}^{-1}$ , the MOT beams are typically detuned by a few linewidths below the atomic resonance, and their  $1/e^2$  radius is 7 mm.

A usual calibration (see for example [16]) of the MOT fluorescence measured on the PM, which takes into account the collection solid angle of the imaging lens and the  $3/7$  average squared Clebsch-Gordan coefficient of the trapping transition, allowed us to estimate the following numbers. Our loading rate is up to  $1.6 \times 10^8$  atoms per second, at an oven temperature of 1500 Celsius. We measured a temperature of  $100 \pm 20 \mu\text{K}$  from the free expansion of the atomic cloud released from the MOT. We obtained a maximum atom number of  $(4 \pm .2 \pm 1) \times 10^6$  [17], corresponding to a peak atom density of  $8 \times 10^{10} \text{cm}^{-3}$  (with a 30% systematic uncertainty).

These results mainly reproduce similar measurements made in the groups of J. McClelland at NIST in Gaithersburg, Ma, USA, and T. Pfau ([11],[16]). First, we observed a strong one-body loss, due to the fact that the cooling transition is not perfectly closed. Atoms in the  $^7P_4$  state can undergo an intercombination transition, which leaves them in either the  $^5D_4$  or the  $^5D_3$  states. These metastable dark states are insensitive to the MOT light, but can remain trapped in the MOT B field gradient. We checked that atoms in these two states can be repumped (via the  $^7P_3$  state), using either one of two single mode extended cavity laser diodes running at 653.97 nm and 663.18 nm, which leads to a slight increase in the total number of atoms in the steady state MOT.

The second striking feature of  $^{52}\text{Cr}$  MOTs is the strong two-body inelastic loss rate, which was measured in [16]. We reproduced the measurements reported in this reference, and found an inelastic loss rate of  $(6.25 \pm .9 \pm 1.9) \times 10^{-10} \text{cm}^3\cdot\text{s}^{-1}$ , when the MOT beams are detuned by 10 MHz from resonance, and have a total intensity of 116  $\text{mW}\cdot\text{cm}^{-2}$ . We briefly describe the experimental

procedure below.

### Magneto-optical Trapping of $^{53}\text{Cr}$ Atoms

The fermionic  $^{53}\text{Cr}$  isotope has already been cooled by collisions with a cold buffer gas [18], but we are the first group to report on properties of the magneto-optical trap of this isotope, which is the first important new experimental result of this paper [19].

The optical manipulation of  $^{53}\text{Cr}$  is not a straightforward extension of the work concerning  $^{52}\text{Cr}$ . The main difference between these isotopes is the complex hyperfine structure of  $^{53}\text{Cr}$ , whose electronic ground state has four different hyperfine components. Although it may be expected that up to three repumpers should be needed to operate the MOT, as well as the ZS, the experiment shows that only two repumpers are needed in the MOT (repumper  $R1$  and  $R2$  in Fig 1), and only one in the ZS. All these repumpers are derived from a single laser beam, using AOMs. In addition to these 'blue' repumpers, three 'red' repumpers are required to prevent atoms from ending up in the metastable states  $|^5D_4, F = 9/2, 11/2\rangle$  or  $|^5D_3, F = 9/2\rangle$ . Due to laser availability when we performed the reported experiments, we were only able to repump atoms from the  $|^5D_4\rangle$  state.

We first achieved a MOT with  $^{53}\text{Cr}$  without any 'red' repumper. Atoms exiting the oven are transversally cooled by a near resonant  $|^7S_3, F = 9/2\rangle$  to  $|^7P_4, F = 11/2\rangle$  laser beam orthogonal to the atom beam, before being decelerated in the ZS. When no transverse cooling is achieved before the atoms enter the ZS, the MOT atom number is reduced by typically 60 percent. As explained earlier, a blue repumping laser detuned by 300 MHz from the slowing transition is mixed with the ZS laser beam to prevent losses at the bad crossing point of the ZS. Typically a few mW is enough for this repumper, and without it the number of atoms in the MOT is only reduced by 30 percent.

The MOT 'blue' beams consist in three different frequencies. The cooling beam is typically detuned by a few linewidths from the atomic transition. Two 'blue' repumpers  $R1$  and  $R2$  respectively correspond to the transition  $|^7S_3, F = 7/2\rangle$  to  $|^7P_4, F' = 9/2\rangle$  and to the transition  $|^7S_3, F = 5/2\rangle$  to  $|^7P_4, F' = 7/2\rangle$  (see Fig 1). No MOT could be obtained without  $R1$ , whereas if  $R2$  is removed, the number of atoms in the MOT is only reduced by 30 percent. We inferred from this observation that repumping on the transition  $|^7S_3, F = 3/2\rangle$  to  $|^7P_4, F = 5/2\rangle$  would not significantly increase the number of atoms in the MOT. The power in  $R1$  and  $R2$  is respectively 10 mW and 3 mW. The  $1/e^2$  radius of the  $^{53}\text{Cr}$  MOT cooling beams is 4.5 mm, and the  $1/e^2$  radius of  $R2$  is 5.2 mm. As for  $^{52}\text{Cr}$ , the MOT magnetic field gradient is 18  $\text{G}\cdot\text{cm}^{-1}$ , and a fluorescence analysis

(with an average squared Clebsch-Gordan coefficient of  $2/5$  for the trapping transition) was used to get quantitative data.

From the depletion rate of the MOT, we estimated the transition probability from  ${}^7P_4$  to the metastable states  ${}^5D_{4,3}$  to be  $280 \text{ s}^{-1}$  (with an uncertainty of 33% mainly of statistical origin) which is significantly higher than the corresponding number for the boson ( $169 \text{ s}^{-1}$ , see Fig 1). We were able to partially cancel these losses with the available 'red' repumper (repumping from the  ${}^5D_4$  state). The steady state atom number in our MOT is multiplied by a factor of 2 in presence of this repumper, and the repumping efficiency saturates for only 2 mW of red light (with a  $1/e^2$  radius of 2.9 mm). No significant increase in the MOT fluorescence was observed when an other red beam, detuned by the 225 MHz hyperfine gap of the  ${}^5D_4$  state shown in Fig 1, was added.

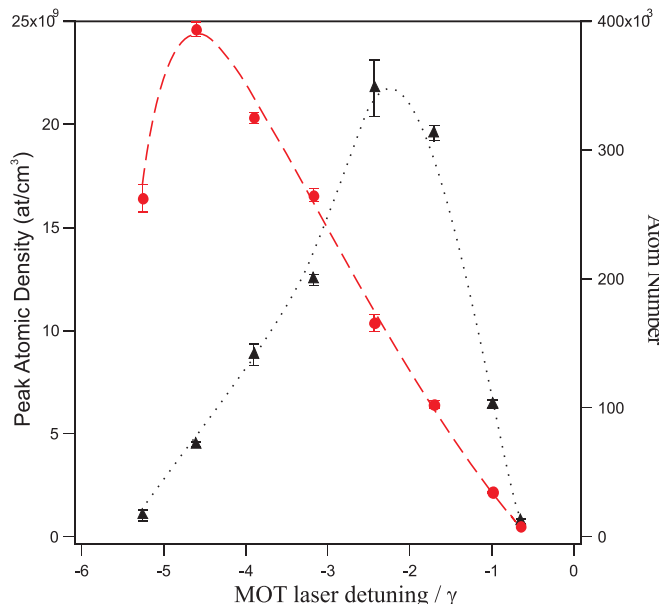


FIG. 3: Atom number (dots) and peak atom density (triangles) in the  ${}^{53}\text{Cr}$  MOT as a function of the normalized detuning of the MOT cooling beam compared to the  $|{}^7S_3, F = 9/2\rangle$  to  $|{}^7P_4, F = 11/2\rangle$  transition, with a total laser intensity of the MOT beams equal to  $200 \text{ mW cm}^{-2}$ . Error bars show the dispersion over 4 data points, and the solid line is a guide for the eye.

We performed systematic studies to measure the total number of atoms in the MOT in presence of the 'red' repumping laser, as a function of the cooling laser intensity and detuning. Figure 3 shows that the MOT atom number and peak density reach a maximum for different values of the MOT laser detunings. We observed up to  $(5 \pm .25 \pm 1) \times 10^5$  atoms in the  ${}^{53}\text{Cr}$  MOT. This steady state number is significantly higher than what is expected from a direct loading comparison with the boson case, if only the relative loading rate (about 2%) and loss rate of the two MOTs are taken into consideration, showing the dramatic effect of inelastic collisions for the denser bosonic

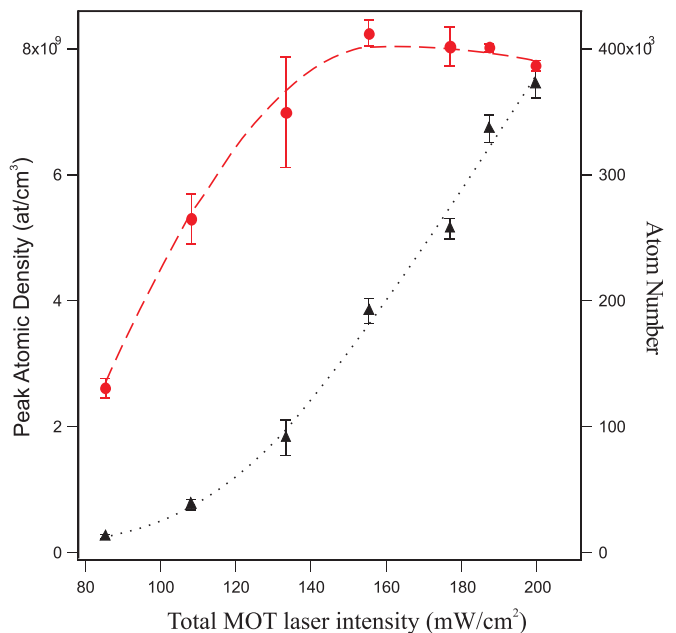


FIG. 4: Atom number (dots) and peak atom density (triangles) in the  ${}^{53}\text{Cr}$  MOT as a function of the total power in the MOT cooling beams, for a detuning of the MOT beams equal to  $-21.5 \text{ MHz}$ . Error bars show the dispersion over 4 data points, and the solid line is a guide for the eye.

MOT. Figure 4 demonstrates a saturation of the MOT atom number with the MOT laser intensity, while the peak density doesn't saturate for the laser power available. The highest peak atomic density obtained was up to  $2.5 \times 10^{10} \text{ cm}^{-3}$  (with a systematic uncertainty of 30%).

Even with one 'red' repumper on, the maximum number of  ${}^{53}\text{Cr}$  atoms in the steady state MOT is below  $10^6$ , which is most likely not sufficient to reach quantum degeneracy via an evaporative cooling procedure. As described below, a very large inelastic rate coefficient in the  ${}^{53}\text{Cr}$  MOT, similar to the one measured for  ${}^{52}\text{Cr}$ , limits the maximum number of atoms in the steady state MOT. Therefore, we studied, similarly to the work reported in [20] for the bosonic isotope, how fermionic metastable atoms can be accumulated in the magnetic trap formed by the quadrupole field of the MOT, before being repumped back into the ground state. A similar accumulation process has been reported for Strontium atoms in [21], but requires a much higher value of the B field gradient.

### Accumulation of ${}^{52}\text{Cr}$ and ${}^{53}\text{Cr}$ Atoms in a Magnetic Quadrupole Trap

Chromium offers a nice way to decouple cooling and trapping: as stated above, atoms are slowly optically pumped into metastable states, whose lifetimes are very large (and unknown), and whose magnetic moments are large enough to be trapped by the MOT gradient mag-

netic field, provided they happen to be produced in a low-field seeking state. In our experiment, we first reproduced the results of [20], and used the same procedure to accumulate metastable  $^{53}\text{Cr}$  atoms in the magnetic quadrupole field of the MOT.

In the case of  $^{52}\text{Cr}$ , the number of trapped metastable atoms saturates in a timescale which is fixed by inelastic collisions with atoms in the excited  $^7\text{P}_4$  state [20]. In the case of  $^{53}\text{Cr}$  MOT, the steady state number of atoms in the  $^7\text{P}_4$  state is about ten times smaller, and we found that the timescale for accumulating  $^{53}\text{Cr}$  metastable atoms in the magnetic trap is set by collisions with fast atoms coming from the oven. It is found to be on the order of 8 s when the oven is operated at 1500 Celsius, which is equal to the measured lifetime of the metastable fermions in the magnetic trap when the atom shutter is not closed (and smaller than the background collision lifetime when the shutter is closed).

By accumulating atoms in the metastable state  $^7\text{D}_4$ , and after repumping them using a 10 ms long 'red' pulse, we measured up to  $(8.5 \pm .4 \pm 2.1) \times 10^5$   $^{53}\text{Cr}$  atoms in the magnetically trapped  $^7\text{S}_3$  ground state. This number was obtained for a detuning of the MOT beams equal to 12.5 MHz, and a total intensity in the MOT beams equal to  $200 \text{ mW.cm}^{-2}$ , which corresponds almost to a tenfold increase compared to the steady state MOT atom number for these parameters. This measurement was achieved close to resonance, and should not correspond to the optimal  $^{53}\text{Cr}$  atom number accumulated in the metastable state (see Fig 3). In addition, such a number was measured by using only one 'red' repumper, and the use of another 'red' repumper for the  $^5\text{D}_3$  state should give us a reasonable starting point for further cold collision experiments, Feshbach resonance studies, and for evaporative cooling down to quantum degeneracy.

This larger number of  $^{53}\text{Cr}$  atoms allowed us to carefully study density dependent losses for the  $^{53}\text{Cr}$  MOT. The two-body loss rate parameter measured for  $^{53}\text{Cr}$  is very large, typically ranging from  $(1 \pm .2 \pm .3) \times 10^{-9}$  to  $(8 \pm .8 \pm 2.5) \times 10^{-9} \text{ cm}^3.\text{s}^{-1}$  for detuning of the MOT laser varying from -20 MHz to -3MHz, and a total MOT laser intensity of  $170 \text{ mW.cm}^{-2}$ . These values are similar to the inelastic loss rates obtained for  $^{52}\text{Cr}$  MOTs. To our knowledge, these very high inelastic loss rates in chromium MOTs are not understood up to now, and will be studied in a forthcoming publication. Here, we note that they are only slightly smaller than the Langevin rate (see [22]).

### Magneto-optical Trapping of a Cold Bose-Fermi Mixture of $^{52}\text{Cr}$ and $^{53}\text{Cr}$ Atoms

In this paper, we report on the first simultaneous magneto-optical trapping of  $^{52}\text{Cr}$  and  $^{53}\text{Cr}$  atoms. To perform this experiment, we make use of a fortuitous

quasi coincidence between two transitions: the cooling transition for  $^{52}\text{Cr}$  and the 'R1' transition for  $^{53}\text{Cr}$ . As a consequence, the cooling beam for  $^{52}\text{Cr}$  is used in the  $^{53}\text{Cr}$  MOT as R1. Another consequence is that the Zeeman repumper of  $^{53}\text{Cr}$  is also simultaneously used as the ZS beam for  $^{52}\text{Cr}$ , so that we do not need a separate AOM to perform the experiment.

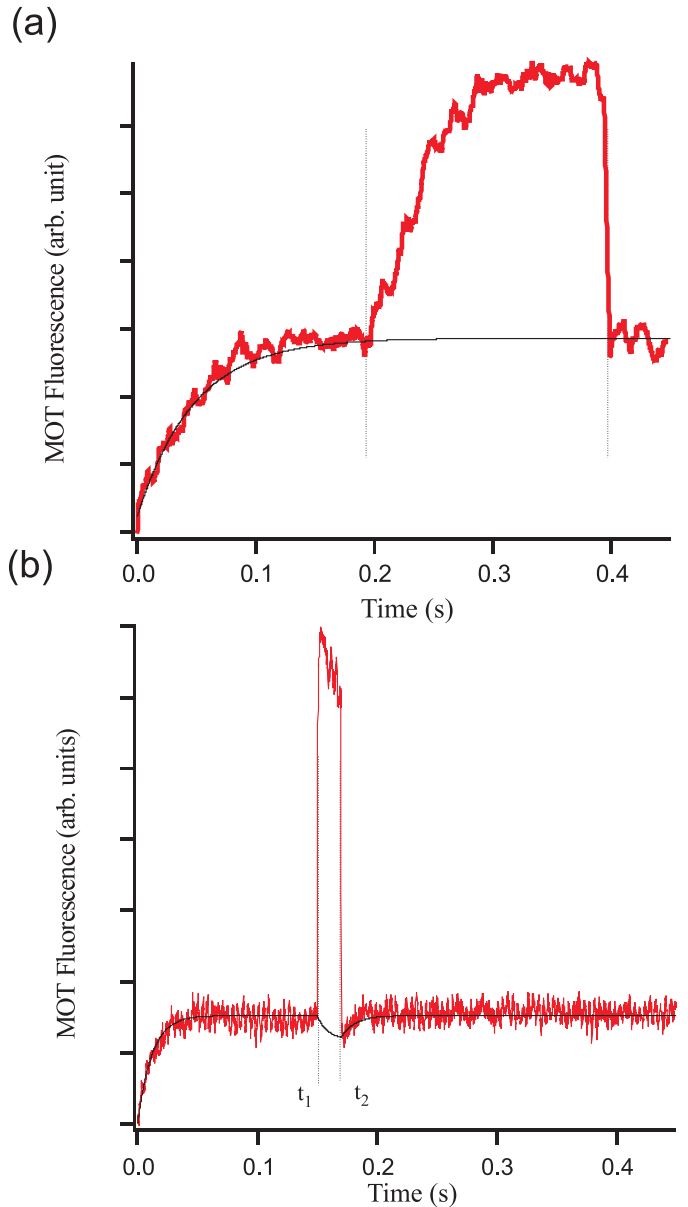


FIG. 5: Loading sequences for simultaneous Magneto-optical trapping of  $^{52}\text{Cr}$  and  $^{53}\text{Cr}$  atoms. The MOT for  $^{52}\text{Cr}$  atoms is turned on at  $t=0$ , whereas the AOMs for the  $^{53}\text{Cr}$  MOT are only turned on during the time period indicated by the two vertical dashed lines. (a) Small number of atoms: when the  $^{53}\text{Cr}$  MOT is turned off, the remaining fluorescence signal of  $^{52}\text{Cr}$  atoms is identical to the one before the  $^{53}\text{Cr}$  MOT was turned on, which means that no mutual effects took place. The solid line is the result of a fit only taking into account fluorescence of bosons. (b) Large number of atoms: after  $^{53}\text{Cr}$  metastable atoms are repumped from the magnetic trap and the large fermionic MOT is superimposed on the  $^{52}\text{Cr}$  MOT, we observe a decrease in the total number of  $^{52}\text{Cr}$  atoms. The solid line is the result of a fit, including interspecies losses.

Figure 5 (a) shows that we can load a  $^{52}\text{Cr}$  MOT, and after it has reached its steady state number, superimpose on it a  $^{53}\text{Cr}$  MOT by simply switching on the AOMs for the cooling transition of the fermion, and  $R2$ . Both MOTs form approximately at the same location according to our CCD fluorescence images. When the  $^{53}\text{Cr}$  MOT laser beams are removed, the number of  $^{52}\text{Cr}$  atoms immediately regains the same steady state value. This demonstrates that neither these lasers nor the presence (in this regime) of  $^{53}\text{Cr}$  cold atoms induce any substantial loss for  $^{52}\text{Cr}$  atoms. However, the data in Fig 5 (a) correspond to very few atoms (about  $3 \times 10^4$   $^{52}\text{Cr}$  atoms, and  $4 \times 10^4$   $^{53}\text{Cr}$  atoms).

In a separate set of experiments, we increased the number of fermionic atoms, by first accumulating them in the trapped metastable states during 10 s. We then loaded a  $^{52}\text{Cr}$  MOT, repumped  $^{53}\text{Cr}$  atoms from the  $^5D_4$  state, thus superimposing about  $7 \times 10^5$  fermionic atoms on the bosonic MOT, with an estimated peak density of fermionic atoms of about  $4 \times 10^{10} \text{ cm}^{-3}$ . We then observed substantial loss of  $^{52}\text{Cr}$  atoms, as shown in Fig 5 (b), which is a proof that fermionic atoms provide a new loss channel for bosonic atoms.

The corresponding loss rate is equal to  $\beta_{BF} \int n_{52}(r)n_{53}(r)d^3r$ , where  $\beta_{BF}$  is the interisotope loss coefficient. If the number of fermionic atoms stays almost constant, this rate, from the bosonic atoms point of view, corresponds to a linear loss rate, being equal to  $\beta_{BF}\bar{n}_{53}N_{52}$ , where  $N_{52}$  is the number of bosonic atoms, and  $\bar{n}_{53} = N_{53}/\bar{V}_{53}$  is an average fermionic density at the bosonic MOT position.  $N_{53}$  is the number of fermionic atoms and  $\bar{V}_{53}$  is a volume depending on the spatial distributions of the two isotopes. Writing the atomic densities as  $n_i(r) = n_{i0}f_i(r)$  gives  $\bar{V}_{53}$  in terms of integrals of the normalized density distributions  $f_i(r)$  ( $i = 52, 53$ ,  $n_{i0}$  is the peak density):

$$\bar{V}_{53} = \frac{\int f_{52}(r)d^3r \int f_{53}(r)d^3r}{\int f_{52}(r)f_{53}(r)d^3r} \quad (1)$$

Experimentally, the MOT density distributions are Gaussian shaped. With the CCD camera we measured the  $1/e$  horizontal and vertical radii of the two MOTs ( $w_{H52} = 110 \mu\text{m}$ ,  $w_{H53} = 150 \mu\text{m}$ ,  $w_{V52} = 110 \mu\text{m}$  and  $w_{V53} = 140 \mu\text{m}$ ), and the small center position separation in between them ( $\Delta z = 60 \mu\text{m}$ , along the vertical axis), with a precision of about 7% for these numbers. From these values the numerical evaluation of the integrals in (1) is straightforward.

For the data in Fig 5, the number of  $^{52}\text{Cr}$  atoms is small enough that we can neglect light assisted collisions among them, so that the evolution equation for the  $^{52}\text{Cr}$  MOT population therefore reads:

$$\frac{dN_{52}}{dt} = \Gamma - \frac{N_{52}}{\tau} - \beta_{BF}\bar{n}_{53}N_{52} \quad (2)$$

where  $\Gamma$  is the loading rate of the  $^{52}\text{Cr}$  MOT,  $\tau$  is the depumping time towards metastable states, and the last term is only present when the fermionic MOT is applied (between  $t_1$  and  $t_2$  in Fig 5 (b)). We fitted the loading sequence of the  $^{52}\text{Cr}$  MOT ( $t < t_1$ ) to deduce  $\Gamma$  and  $\tau$ . We then adjusted  $\beta_{BF}$  to reproduce the reduction of  $^{52}\text{Cr}$  atoms when the  $^{53}\text{Cr}$  MOT is removed at  $t = t_2$ . From this analysis (similar to the one performed for a K-Rb MOT in [23]), we estimated the light assisted inelastic loss coefficient between  $^{52}\text{Cr}$  and  $^{53}\text{Cr}$  to be  $\beta_{BF} = (1.8 \pm .45 \pm .65) \times 10^{-9} \text{ cm}^3.\text{s}^{-1}$ , for  $^{52}\text{Cr}$  ( $^{53}\text{Cr}$ ) MOT beams detuned by 10 (12.5) MHz, and having a total intensity of 70 (200)  $\text{mW.cm}^{-2}$ . The solid line in Fig 5 (b) is the result of our numerical fit.

$\beta_{BF}$  is on the same order of magnitude than the light assisted loss coefficient that we measured both in a  $^{52}\text{Cr}$  MOT and in a  $^{53}\text{Cr}$  MOT. However, physics of light assisted collisions in the case of a mixture is different than for a single-species MOT. For homonuclear molecules, the long range part of the excited molecular potential asymptotically related to the  $(S, P)$  dissociation limit is dominated by resonant dipole-dipole interaction, scaling as  $C_3/R^3$ . In contrast, for heteronuclear molecules, the excited molecular potential is dominated by a Van-der-Waals interaction scaling as  $C_6/R^6$  ([24]). Thus, in a MOT composed of two different species, inter-species light-assisted collisions typically occur at shorter inter-atomic distances than intra-species light assisted collisions. In addition, the  $C_6$  coefficient for the molecular potentials related to the ( $^{52}\text{Cr}, ^7S_3$ ,  $^{53}\text{Cr}, ^7P_4$ ) dissociation limit is positive. The associated molecular potentials are repulsive and should not lead to light assisted losses in a MOT (as discussed in [24]). Therefore, we interpret losses related to light assisted collisions in our double MOT as the consequence of a process involving molecular potentials related to  $^{52}\text{Cr}, ^7P_4$  and  $^{53}\text{Cr}, ^7S_3$ . However, because the shift between the cooling transitions for  $^{52}\text{Cr}$  and for  $^{53}\text{Cr}$  is small, the situation may be more complicated, because the molecular excited potentials should be in  $1/R^6$  at large distance, with a very large  $C_6$ , and in  $1/R^3$  at shorter distances. This situation is similar to dipole-dipole interactions in cold Rydberg gases [25].

A complication for continuously collecting large numbers of atoms in our mixed-species MOT arises from the fact that the  $^{52}\text{Cr}$  MOT is substantially altered by the presence of the  $^{53}\text{Cr}$  ZS beam. We attribute this effect to the fact that slowed  $^{52}\text{Cr}$  atoms are pushed by the  $^{53}\text{Cr}$  Zeeman slower beam as they approach the MOT region (as the ZS magnetic field goes to zero, the bosonic atoms slowly travel through a region where they are resonant with the  $^{53}\text{Cr}$  ZS laser frequency). Our observations suggest that the best strategy to obtain large samples of cold  $^{53}\text{Cr}$  and  $^{52}\text{Cr}$  atoms is to sequentially accumulate them in the metastable states, before repumping both isotopes in their electronic ground state.

## CONCLUSION

We have reported the magneto-optical trapping of cold fermionic  $^{53}\text{Cr}$  atoms. Magnetic trapping of metastable atoms in the quadrupole field of the MOT was demonstrated, yielding an increase in the number of atoms by a factor of seven. These features are encouraging as a first step in producing a degenerate dipolar fermi gas. Furthermore we demonstrated the achievement of a dual-isotope boson-fermion MOT. This opens the way to two isotope collision studies, including the search for inter isotope Feshbach resonances, and the obtention of sympathetic cooling. It also opens the way to the potential realization of a quantum degenerate boson-fermion mixture involving dipolar species.

Acknowledgements: LPL is Unité Mixte (UMR 7538) of CNRS and of Université Paris Nord. We acknowledge financial support from Conseil Régional d'Ile-de-France (Contrat Sesame), Ministère de l'Education, de l'Enseignement Supérieur et de la Recherche, and European Union (FEDER - Objectif 2). We also thank C. Chardonnet, V. Lorent and H. Perrin for their help in starting this project, as well as J. McClelland and T. Pfau for their many friendly advices.

- 
- [1] H. J. Metcalf and P. van der Straten, *Laser Cooling and Trapping*, Springer (1999)
- [2] A. Griesmaier et al. *Phys. Rev. Lett.* **94** 160401 (2005)
- [3] J. Stuhler et al. *Phys. Rev. Lett.* **95**, 150406 (2005)
- [4] B. Brezger et al., *J. Vac. Sci. Technol. B* **15**(6) Nov/Dec 1997, W. R. Anderson et al., *Phys. Rev. A*, **59**, 2476 (1999)
- [5] S. J. Rehse et al. *Appl. Phys. B.*, **70**, 657 (2000), B. Smeets et al. *Appl. Phys. B.*, **80**, 833 (2005).
- [6] B. De Marco and D. S. Jin, *Science* **285**, 1703 (1999), F. Schreck et al., *Phys. Rev. Lett.* **87**, 080403 (2001), A. G. Truscott et al., *Science* **291**, 2570 (2001), S. R. Granade et al., *Phys. Rev. Lett.*, **88**, 120405 (2002).
- [7] M.A. Baranov et al *Phys. Rev. Lett.* **92**, 250403 (2004)
- [8] T. W. Hänsch and B. Couillaud, *Optics Comm.*, **35**, 3, 441 (1980)
- [9] J. Stuhler, Ph.D thesis, Universität Konstanz (2001)
- [10] W. Ertmer et al. *Z. Phys. A - Atoms and Nuclei*, **309**, 1 (1982), T. Reinhardt et al. *Z. Phys. D.* **34**, 87 (1995)
- [11] A. S. Bell et al. *Europhys. Lett.* **45** (2), 156-161 (1999)
- [12] R. Drever et al *Appl. Phys. B* **31** , 97 (1983)
- [13] P.A. Molenaar et al., *Phys. Rev. A*, **55**, 605 (1997)
- [14] C. Slowe et al., *Review of Scientific Instruments*, **76**, 103101 (2005)
- [15] A direct coupling through a viewport must be avoided because the atomic chromium beam would rapidly coat it; J. McClelland and T. Pfau, personal communications.
- [16] C. C. Bradley et al. *Phys. Rev. A* **61**, 053407 (2000)
- [17] In this paper, error bars correspond successively to the statistical and the systematic uncertainty, except otherwise stated.
- [18] Cold  $^{50}\text{Cr}$ ,  $^{52}\text{Cr}$ , and  $^{53}\text{Cr}$  atoms, at temperatures as low as 10 mK, were also obtained in the group of J. Doyle: the atoms were magnetically trapped, after being sympathetically cooled by a cryogenic helium buffer gas. See J. D. Weinstein et al., *Phys. Rev. A* **65**, 021604(R) (2002).
- [19] A few years ago, the group of T. Pfau made preliminary observations of a  $^{53}\text{Cr}$  atoms magneto-optical trap (private communication, and [9]).
- [20] J. Stuhler et al., *Phys. Rev. A* **64**, 031405 (2001), P. O. Schmidt et al. *J. Opt. B: Quantum Semiclass. Opt.* **5** (2003) S170-177.
- [21] S.B. Nagel et al., *Phys. Rev A* **67**, 011401 (2003)
- [22] P. S. Julienne and J. Vigué, *Phys. Rev. A*, **44**, 4464 (1991)
- [23] L. G. Marcassa et al., *Phys. Rev. A* **63**, 013413 (2000)
- [24] U. Schlöder et al., *Eur. Phys. J. D* **7**, 331 (1999).
- [25] W. Li et al. *Phys. Rev. Lett.* **94**, 173001 (2005)